Naval Research Laboratory
Washington, DC 20375-5320

NRL/MR/7120--97-7956

Transmission Loss and Frequency-Angle-Time Spread: Issues and Model Analysis for the Littoral Warfare Advanced Development Focused Technology Experiment 96-1

T.C. YANG
A. AL-KURD

Acoustic Signal Processing Branch
Acoustics Division

T. YATES

Vector Research Corporation
Rockville, Maryland

May 27, 1997

REPORT DOCUMENTATION PAGE

Form Approved
OMB No. 0704-0188

1. AGENCY USE ONLY (*Leave Blank*)	2. REPORT DATE	3. REPORT TYPE AND DATES COVERED
	May 27, 1997	Memorandum

4. TITLE AND SUBTITLE

Transmission Loss and Frequency-Angle-Time Spread: Issues and Model Analysis for the Littoral Warfare Advanced Development Focused Technology Experiment 96-1

5. FUNDING NUMBERS

PE - 06037447N

6. AUTHOR(S)

T.C. Yang, A. Al-Kurd, and T. Yates

7. PERFORMING ORGANIZATION NAME(S) AND ADDRESS(ES)

Naval Research Laboratory
Washington, DC 20375-5320

8. PERFORMING ORGANIZATION REPORT NUMBER

NRL/MR/7120--97-7956

9. SPONSORING/MONITORING AGENCY NAME(S) AND ADDRESS(ES)

Office of Naval Research Code 32
Arlington, VA 22217-5660

10. SPONSORING/MONITORING AGENCY REPORT NUMBER

11. SUPPLEMENTARY NOTES

12a. DISTRIBUTION/AVAILABILITY STATEMENT

Approved for public release; distribution unlimited.

12b. DISTRIBUTION CODE

A

13. ABSTRACT (*Maximum 200 words*)

A mid-frequency active system concept was tested during the Focused Technology Experiment (FTE 96-1) sponsored by the Littoral Warfare Advanced Development (LWAD) program. Specifically, the BSDS directional projector was used as the source, an echo repeater was used to simulate the target, and the MUF (multiple frequency) volumetric array was used as the receiver. This report discusses modeled frequency, angle, and time spreading associated with one-way transmission loss, using the environmental parameters measured during the at-sea test. This modeling is intended to provide environmental acoustic support for the interpretation of the observed active detection performance and to help guide measurements made in future tests. We address issues such as source-receiver range and depths, propagation environments that impact the measurements of the transmission loss at mid frequencies in shallow waters, the difference in transmission loss using an omni-directional source versus that of a directional source (as used in some systems), the difference in model prediction between a normal mode and a PE model and its implications, and the advantages of using a continuous wave (CW) signal versus a broadband signal in the measurements of transmission loss and channel transfer function. These issues need to be examined for each experiment. Understanding of these issues with support from numerical analysis will significantly improve the quality of the data collection and help data interpretation. Candidate broadband signal waveforms and data analysis approach are discussed in an Appendix.

14. SUBJECT TERMS

Transmission loss
Frequency-angle-time spread
Channel transfer function
Underwater acoustics

15. NUMBER OF PAGES

32

16. PRICE CODE

17. SECURITY CLASSIFICATION OF REPORT	18. SECURITY CLASSIFICATION OF THIS PAGE	19. SECURITY CLASSIFICATION OF ABSTRACT	20. LIMITATION OF ABSTRACT
UNCLASSIFIED	UNCLASSIFIED	UNCLASSIFIED	UL

NSN 7540-01-280-5500

Standard Form 298 (Rev. 2-89)
Prescribed by ANSI Std 239-18
298-102

CONTENTS

ABSTRACT 1

1. INTRODUCTION 2

2. EXPERIMENTAL MEASUREMENT 4

   2.1 TL for a Line Source versus a Point Source 4
   2.2 Up Slope, Down Slope versus Across Slope 5
   2.3 TL versus Range 5

3. TL AND FAT MODELING 6

   3.1 Sensitivity of TL to Measured Sound Speed Variations 7
   3.2 TL for a Line Source versus a Point Source 8
   3.3 Frequency-Time Analysis of a Broadband HFM Pulse 8
   3.4 Comparisons of Model Predictions 9

4. SUMMARY 9

5. ACKNOWLEDGMENT 10

6. REFERENCES 10

APPENDIX 29

Transmission Loss and Frequency-Angle-Time Spread: Issues and Model Analysis for the Littoral Warfare Advanced Development Focused Technology Experiment 96-1

T. C. Yang and A. Al-Kurd

Naval Research Laboratory

Washington, DC 20375

T. Yates

Vector Research Corporation

2101 Jefferson St., Rockville, MD 20852

Abstract

A mid-frequency active system concept was tested during the Focused Technology Experiment (FTE) 96-1 sponsored by the Littoral Warfare Advanced Development (LWAD) program. Specifically, the BSDS directional projector was used as the source, an echo repeater was used to simulate the target and the MUF (multiple frequency) volumetric array was used as the receiver. This report discusses modeled frequency, angle, and time spreading associated with one-way transmission loss, using the environmental parameters measured during the at-sea test. This modeling is intended to provide environmental acoustic support for the interpretation of the observed active detection performance and to help guide measurements made in future tests. We address issues, such as source-receiver range and depths, propagation environments, that impact the measurements of transmission loss at mid frequencies in shallow waters, the difference in transmission loss using an omni-directional source versus that of a directional source (as used in some systems), the difference in model predictions between a normal mode and a PE model and its implications, and the advantages of using a continuous wave (CW) signal versus a broadband signal in the measurements of transmission loss and channel transfer function. These issues need to be examined for each experiment. Understanding of these issues with support from numerical analysis will significantly improve the quality of the data collection and help data interpretation. Candidate broadband signal waveforms and data analysis approach are discussed in an Appendix.

Manuscript approved May 19, 1997.

1. INTRODUCTION

A series of Focused Technology Experiments (FTE), under the Littoral Warfare Advanced Development (LWAD) program, sponsored by the Office of Naval Research, are conducted each year to address the science and technology issues that impact the performance of several system concepts that have high potential of transition to fleet systems. During the FTE-96-1 experiment, the performance of a mid-frequency active system using a directional source, an echo-repeater, and a volumetric array was evaluated among other projects.

To evaluate the system performance either during the sea tests or in post experiment analysis, one needs to know the signal transmission loss (TL) from the source to the receiver. In addition, one needs to investigate the frequency-angle-time spread of a signal which can result in a degradation of the system performance. The environmental effects on signal propagation has been extensively researched in deep water. In shallow water, at mid (tactical) frequencies, the subject is not well studied. As the Navy interest moves into shallow waters, it behooves us to address these issues systematically.

Shallow water differs from deep water in many aspects. The sound interacts more with the surface and bottom in shallow water, hence the surface roughness and bottom sediment affect the TL and signal coherence. The water column is complex in shallow water, due to intrusion of fresh water and/or shelf/slope water, ocean (gulf) currents, eddies and meanders of boundary currents, tidal waves, etc. Previous studies have shown that sound propagation is significantly influenced by the internal waves and fine/micro-fine inhomogeneities in the ocean created by the various oceanographic processes. These processes introduce not only spatial dependence but also temporally fluctuation in the sound channel.

Multipath arrivals and frequency dispersion of the waveguide are responsible for the signal spread in time; an effect that is particularly important in shallow water. Depending on the bottom reflectivity, attenuation, water depth, and sound speed profile, there may be few or many bottom-bounce returns. The number of bottom-bounce returns determines the length of the received pulse (train). In shallow water, the individual bottom-bounce often can not be clearly identified in the received times series; the overlapping of the arrivals changes the signal waveform. At high frequencies, signal waveform can be significantly smeared and distorted by scattering from the rough surface and bottom. At low frequencies, the signal waveform may exhibit strong frequency dispersion, the received waveform will contain wave packets traveling with modal group velocities. For a signal with wide bandwidth, the signal waveform can be modified by the frequency dependence of the bottom reflection loss. As a consequence of these factors, the received waveform could differ significantly from the emitted waveform in shallow water. Significant waveform distortion will reduce the matched filter processing gain and degrade the performance of an active system.

Multipath arrivals can cause the signal to appear in more than one vertical and/or horizontal beam. The angle spread of the multipath arrivals will degrade the signal gain if the angle spread is larger than the beam width. The energy split of the signal degrades the signal gain.

Platform Motion can cause a Doppler shift of the received signal. Doppler shift is an important parameter to be estimated from the data, but the measurement can be smeared by frequency

spread caused by the reflection/scattering of the signal from a time-varying ocean surface. Significant frequency spread may also affect system performance.

In this report we shall concentrate on the issues affecting the transmission loss and channel transfer function. We have studied these issues using two propagation models (normal mode and PE) assuming a deterministic ocean (a common practice for transmission-loss modeling). The inputs to the acoustic model are the sound-speed profile, density, and attenuation. The input parameters are taken from an environmental survey for the water column and bottom. The model calculates the acoustic pressure field at the receivers, from which one deduces the signal transmission loss and the channel transfer function. From the channel transfer function, one can derive the time and angle spread of a broadband (HFM or LFM) signal.

There are two issues regarding the modeling work. The first issue concerns the adequacy of the environmental parameters. The second issue concerns with how well the modeling result compare with data. When comparing an acoustic model with data, one often has the freedom that a few parameters can be adjusted to fit the data. For a temporally and spatially varying environment representing a random medium, the stochastic nature of the signal is an important factor to consider when comparing measured data with model results. In that case, the acoustic model must incorporate not only the deterministic mean value but also the variance in the signal due to propagation in the random medium. These issues point out that TL/FAT modeling in shallow water is non-trivial at mid-frequencies (several hundred Hertz to 10 kHz). To our knowledge, prior work for modeling the TL at mid frequencies followed mostly the approach of acoustic ray tracing. To model the channel transfer function properly, we use a full field model such as the normal mode or parabolic equation model. These models have been extensively benched marked and compared with data at low frequencies. The same effort is somewhat lacking at mid frequencies.

A well recognized fact is that one cannot depend on acoustic modeling alone nor on data alone for system design and performance prediction. Usually, the available data is limited and the acoustic models may not agree with data. The data may be obtained under oceanographic environments which are different from the ones of interest. This sets the stage for the TL analysis. The objective of acoustic modeling and data analysis should be to investigate and evaluate the degree of confidence for signal and noise properties (parameters) prediction. An acoustic model with results that agree with most of the measured data should be of value to the system analysis community.

An effort is being made in the LWAD series of experiments to collect experimental data on TL and FAT spread using several signal waveforms. The TL and FAT data will be analyzed to compare with acoustic model predictions. The TL modeling will be performed initially to guide the TL experiment and later to compare with data. The modeling results can be used to study the sensitivity of the model predictions to the environmental and source/receiver parameters. After the acoustic model has been validated against data with some confidence, the model can be used by investigators to predict TL and FAT for their experimental runs. In some cases, the numerical values predicted may not be correct, but it should at least help the investigators in understanding the data and interpreting the system evaluation results.

The various signal waveforms to be used in the LWAD experiments are described in Appendix A. Matched filter processing of the broadband signals is presented to show the data analysis approach

for deducing the TL and channel impulse response from the received signals and the advantages offered by broadband signals.

2. EXPERIMENTAL MEASUREMENT

During the FTE 96-1 experiment, the TL and FAT measurements were performed using the Naval Air Warfare Center BSDS directional source and Multi-frequency (MUF) receiver array which are components of the research ALFS system. Various types of broadband waveforms were transmitted by the BSDS source. The signals were received by the Echo Repeater and the echo return from the Echo Repeater were received by the MUF array. Using the signal received by the Echo Repeater one investigates the one-way transmission loss. Using the signal received by the MUF one can study the two-way transmission loss.

FTE 96-1 was a wet-down test. The Echo Repeater could not automatically trigger and transmit the received signal. There were very limited data collected during this experiment for TL analysis. In this report we will use modeled TL/FAT results to discuss many of the technical issues one would address when data are available.

Note that the BSDS is a line source, not a point source, with a beam pointed to the broadside direction. Since transmission loss normally refers to the energy loss of a signal from an omni-directional source, the data are not directly applicable. The data measured using the line source is applicable to the ALFS system analysis. With the source level defined at 1 m in the broadside direction, one can define a transmission loss as the difference of the received level (on a signal phone) and the source level. This transmission loss will be called the "system" transmission loss.

2.1 TL for a Line Source versus a Point Source

A question asked by the LWAD community is "Can one determine the system TL from the omni-directional TL?" Conversely "Can one measure the omni-directional TL from the TL data of a vertical line source?" This is a question of practical importance since a line source projects more energy than an individual (omni-directional) transducer in the array (assuming the same voltage to all transducers). For the TL measurement, a high level source will be needed since an adequate signal-to-noise ratio (e.g., > 5 dB) is required for TL measurements. A higher source level is needed for an active system since it involves two way TL. A highly directional source is often beneficial for reduction of reverberation.

To answer the above questions, one needs to study how a target is insonified by a vertical line source versus an omni-directional source. The line source is characterized by the on-axis (broadside) source level and the vertical beamwidth. If the vertical beamwidth is wide enough such that it insonifies all the important source-receiver paths equally, then the distinction between the line source and omni-directional source disappears except for the source level. If the directivity of the source over-resolves the different propagation paths, then the target insonification will be different for a line source than for an omni-directional source. For the line source, the target insonification depends on whether the target lies on the path covered by the acoustic ray associated with the on-

axis beam. If this is not the case, then the target will be less insonified than would have been by an omni-directional source of equal source level.

We use the propagation model to compare the target insonification of a vertical line source versus an omni-directional source. In the model, the line source transducers are coherent, the on-axis source level is 20 log N of the individual source, where N is the total number of transducers on the line source. To deduce the TL for the line source in the numerical model, one would calculate the acoustic field from each source on the line array, coherently sum the field and then remove 20 log N (dB) from the received level in the line source case. The result can then be used to check the difference of the TL between the line source and the omni-directional source. Based on the acoustic modeling presented below, one finds that the TL from an omni-directional source and the line-source data are approximately the same for most of the receiver locations. In practice, we note that the on-axis line-source level is probably less than 20 log N of the source level of a single transducer. The actual on-axis source level thus needs to be measured.

2.2 Up Slope, Down Slope versus Across Slope

The next question is "Should one conduct the TL/FAT measurements across the slope or down/up the slope?" In order to support the technical evaluation of the system, TL measurement and calculations should be performed for all plausible geometries with respect to slopes. Since it is usually impossible to exhaust all the combinations (especially with bistatic systems) experimentally, one needs to resort to TL calculations for the test geometries where there is no data. Hence, the measurement requirements are to ensure that the TL model can be quantitatively defined and the TL calculations are believable. In other words, a right subset of the large range of possible TL measurements are made so that one can extrapolate/calculate TL with some confidence. In the case of complex environments, it may be useful to provide baseline (simple environment) values and probable ranges of deviation (up and down) of TL from the baseline that we would expect the complexity to produce.

When experimental resources (ship time) are limited, it is recommended that the TL and FAT measurements should be conducted in an acoustic environment with as little range-dependence as possible. The purpose here is to remove any propagation effects due to the bathymetry change which could complicate the issues in the comparison of data with acoustic model predictions. A range-independent environment offers a better chance for the model parameters to be determined from the data. In applying the acoustic model to a range dependent environment (e.g., when the system data are collected), we note that the sound-speed profiles can vary with time and location of each experimental run. Hence adequate temporal and spatial sampling of the sound-speed profiles over the propagation path will be required. The same applies to the bottom properties if they change significantly with range. How sensitive the TL and FAT results are to the sound-speed variations during the period of the experiment will be of interest to the system analysts.

2.3 TL versus Range

A third question is "How far in range does the TL measurement need to be conducted?" This is a valid question since long-range TL measurement requires more ship time and higher source level. For the purpose of system evaluation, TL should be measured to a range where detection is

expected by the system. But often, TL needs to be measured in order to determine the detection range (with confidence). From the point of view of TL modeling, one notes that short-range TL data can often be fitted with several models. TL needs to be measured to a range where the model can be validated with certain degree of confidence. The reasons for extended range are two: First, TL data fluctuate with range. Comparison between data and model require range-averaging of the data and model results. Second, TL depends on bottom attenuation and surface/bottom scattering. The difference between models is statistically meaningful (i.e., greater than the RMS fluctuation in the data) only at long ranges. Still, how long a range does one need to conduct the TL run? The answer depends mostly on the bottom attenuation. Typically one needs to go as far as 20 km. Another rule of thumb will be to measure TL until TL reaches a certain value, say, 90 dB. The range issue can be investigated using TL models prior to the experiment.

Would it be sufficient to measure TL only at long ranges, e.g., 10 to 20 km? It is better to also have short-range data in order to verify the result. At short ranges, the loss is spherical to cylindrical. Short-range data can be used to check the data, such as whether the source and receiver calibrations are correct.

3. TL AND FAT MODELING

We modeled the broadband transmission loss and frequency/time spread of broadband signals using waveforms transmitted by the BSDS source. For transmission loss, we averaged the TL in intensity over the frequency band of the transmitted signals. In this section, we show the modeled TL and FAT results. We plot the field distribution of the acoustic signals at a fixed frequency, then, we plot the TL as a function of range for two source depths, 30.5 m and 76.2 m (100 ft. and 250 ft) and for two receiver depths, 18.3 m and 79.3 m (60 ft and 260 ft) for both an omni-directional source and a line-source. We also plot the matched filtered (time series) output of a HFM signal received by an omni-directional receiver, and its time/frequency spread. We note that the output of a stave of the MUF receiver array is equivalent to a broadside beam pointed to a near horizontal direction. As such, the angle spread of the vertical arrivals is not a critical issue and is not modeled. The MUF has a reasonably wide vertical beamwidth.

For acoustic modeling of the TL/FAT, we need to be aware of two things. First, the TL depends on the sound-speed profile which, in a dynamic area, could change rapidly with time. Second, the TL modeling results may differ for the same environmental acoustic inputs, depending upon what model (e.g., normal mode versus PE) one uses, and what parameters one sets in running the model (e.g., range/depth integration cell). For these reasons, one cannot over-emphasize the need for comparison of model results with experimental data if one intends to have a prediction capability. In this report, we will run numerical results to shed light on these two issues.

There are two possible scenarios in addressing the first issue. For certain environments one could find that the TL varies little (less than 2 dB) within the range of the sound-speed changes, Then the TL modeled based on the sound-speed profile collected will most likely be adequate for system evaluation. On the other hand, if the TL changes significantly with the sound-speed changes found in a certain area, one must measure the sound-speed profile for each test and use that sound-speed profile for that particular test only. The lessons learned in the comparisons of data versus model in a particular area would likely apply to a Navy system operating in that area.

3.1 Sensitivity of TL to Measured Sound Speed Variations

The question of the TL variability is investigated here using three sound-speed profiles measured during the experiment. The results presented below use a normal mode program called Modelab developed by the Applied Research Laboratory at the University of Texas[1]. The measurement of the sound-speed profiles in the water column and bottom properties has been previously addressed in Ref. 2. In Ref. 2, the sound-speed profiles are categorized into three groups. For our study, we chose three sound-speed profiles that were collected during the period designated for the ALFS that adequately cover the range of sound-speed changes reported in Ref. 2.

The three sound-speed profiles are plotted in Fig. 1. The first profile (with bottom depth of 938 m) was collected at 27.95 N and 78.67 W on 23 April 96 about 11 PM local time. The second profile (with bottom depth 913 m) was collected at 28.10 N and 78.75 W on 24 April 96 about 9 AM local time. The third profile (with bottom depth of 892 m) was collected at 27.89 W and 78.77 on 24 April 96 about 5 PM local time. One observes that the largest sound-speed change occurred at depths between 400 and 800 m. The sound-speed can change by as much as 10 m/s. How does the sound-speed changes affect TL measurements and predictions?

To illustrate the dependence of TL on the sound-speed profiles, we plot in Figs. 2-4 the acoustic field as a function of receiver depth and range using the three sound-speed profiles for an omni-directional source at depth of 30.5 m (100 ft) The ocean bottom is modeled as given in Ref. 2. For illustration, we use an acoustic frequency of 3380 Hz. We observe that the field distributions in the three plots are similar, but there are differences in the details.

The differences in the received level are shown by plotting the modeled TL as a function of range. The receiver is at a depth 18.3 m (60 ft) and 79.3 m (260 ft) in Fig. 5A and 5B, respectively. The TL curves are averaged over a bandwidth of 280 Hz for a better representation of the TL results.

We note that for the receiver at depth of 18.3 m (60 ft) (Fig. 5A), the sound-speed variations have an insignificant effect on the average TL for source-receiver ranges less than 1.6 km, and between 6 and 10.5 km. For ranges between 1.6 and 6 km, the receiver is in the shadow zone which is shown in Figs. 2-4. The extent of the shadow zone and the degree of the shadowing effect depend on the sound-speed profile as well as the water depth. The water column differs as much as 46 m between the three environments. For ranges beyond 10.5 km, the TL can differ by several (e.g., 5) dB between the environments.

Figure 5B shows that for a receiver at depth of 79.3 m (260 ft), the average TL is insensitive to the sound speed variations when the receiver is at ranges less than 2 km or between 6 and 12 km from the source. When the receiver is between 3 and 5.5 km from the source, it is in the shadow zone and the average TL level varies by more than 5 dB depending on the sound-speed profile being used. When the receiver is at ranges greater than 12 km, the acoustic field contains two or more bottom-bounce arrivals. The difference in the acoustic field (due to sound-speed variations) starts to accumulate among the various bottom-bounce arrivals. This is reflected in the average TL as well as the interference pattern (the oscillation of the intensities with respect to range).

Comparing Fig. 5A with 5B, we note that the average TL to a receiver at 18.3 m (60 ft) or 79.3 m (260 ft) depth is approximately the same when the receiver is outside the shadow zone.

Figures 6-8 plot the field intensity as a function of range and depth for the three environments mentioned above with the source at a depth of 76.2 m (250 ft).

Figures 9A and 9B plot the TL for a receiver at depth of 18.3 m (60 ft) and 79.3 m (260 ft) respectively. Again, we note that the TL is insensitive to the sound-speed variations at receiver range less than 2 km and between 6 and 10 km.

3.2 TL for a Line Source versus a Point Source

The above results are TL from a point source. Next we would investigate TL for a line source of 8 identical transducers. This source has a maximum (on-axis) response in the broadside direction. The (maximum) on-axis source level of a line source is 18 dB (20 log 8) higher than an individual source, since all transducers are in phase. The beam pattern of this line source enhances low grazing angle acoustic rays and suppresses high grazing angle acoustic rays at the source. In contrast, an omni-directional source emits acoustic rays at all angles. In terms of the normal modes, the low order modes are excited more by the line source than the omni-directional source. Hence it is not apparent if the acoustic field distribution will be the same with the line source as with an omni-directional source.

The field intensity for a line source is calculated by coherently summing the fields from 8 individual sources. The sound-speed profile No. 2 of Fig. 1 is being used. The field intensity, reduced by 18 B (20 log 8), is compared with that from one source located at the center of the line-source. The difference (in dB) between the normalized intensity of the line-source and single source is plotted in Fig. 10. For this simulation half wavelength spacing is assumed between the elements in the line-source. The source is at a depth of 30.5 m (100 ft). One can identify in Fig. 10 a field distribution corresponding to acoustic ray trajectories. We find that the difference between the field intensities is negligible (< 2 dB) for range-depth cells covered by acoustic rays of grazing angles less than ~24^{o} (the beamwidth of the line array). On the other hand, where the acoustic field is propagated only by steep acoustic rays, the difference between the field intensities could be as high as 10 dB. One notes that the field intensities along the deep angle (> 30^{o}) acoustic rays are less for the line array source than for the omni-directional source. This result is not surprising due to the different beam patterns of the source as remarked earlier.

The above analysis basically says that we can use a line source such as the BSDS to conduct the TL measurements, but the results need to be translated into the conventional TL by adjusting (calibrating) the field distribution as shown in Fig. 10. A comparison test of TL data from an omni-directional source and a vertical line-array source needs to be conducted first.

3.3 Frequency-Time Analysis of a Broadband HFM Pulse

Figure 11 shows the matched-filter output of a broadband, HFM, signal with ~200 Hz bandwidth and duration of 512 ms projected by a vertical line source (Fig. 11A) and the same matched-filter output for the signal received by a hydrophone at a range of 10 km (Fig. 11B). The receiver is at a depth of 30 m (98.4 ft). The spectrum of the signal and its time-frequency dispersion are also shown at the source and receiver location. The result indicates that the multipath structure is not

severe for a broadband signal at ~3.5 kHz since the signal is practically dominated by a single path. This observation is specific to this environment and should not be generalized to other oceans. Within the same environment, the multipath structure in the received signal will still be dependent on the source and receiver depth. Details of broadband signal processing are given in Appendix A.

3.4 Comparisons of Model Predictions

Next we investigate the TL using a different propagation model. We have presented the normal mode results above. We now use the University of Miami (UMPE) model[3]. Sound-speed profile No. 3 is used for this simulation. Figures 12A and 12B show the UMPE TL for a source at depth of 30.5 m (100 ft) and two receivers at depths of 18.3 m and 79.3 m (60 ft and 260 ft). Figures 13A and 13B show the TL for a source at 76.2 m (250 ft) depth with the same receivers. Comparing Figs. 12 and 5 using the mean (i.e., range-averaged) TL values, we note that there is an overall agreement in the TL calculation between the two models, but there are also substantial differences at some receiver ranges, particularly the absence of shadow zones in the UMPE results. Similar observations are found when Figs. 13 is compared with Figs. 9. Note that each model contains approximations. The normal-mode model ignores the continuum contribution which is included in the PE calculation. Usually, the continuum is negligible except at short ranges. The PE model uses approximations for high-angle propagation. Both the normal-mode and PE models have been extensively compared with data at low (< 1 kHz) frequencies. Relatively little comparison with data has been made at mid-frequencies. LWAD provides an opportunity to conduct this research.

4. SUMMARY

Transmission loss (TL) and the frequency-time spread of a broadband HFM signal have been modeled in this report to support system performance analysis during the FTE 96-1 experiment. The frequencies and the source and receiver configuration correspond to that used by the MUF/BSDS system. Using acoustic propagation models, we have addressed the technical issues related to the TL measurements, the TL dependence on the sound-speed profile, the validity of numerical models, and the need for comparison of models with TL data.

The normal-mode predictions for TL indicated that using the sound-speed profiles measured during the experiment, the average TL (for an omni-directional source) for a source at a depth of 30.5 m (100 ft) or 76.2 m (250 ft) and a receiver at a depth of 18.3 m (60 ft) or 79.3 m (260 ft) is approximately the same when the source-receiver range is less than 2 km or between 6 and 10 km. This result is valid for all three sound speed profiles used which implies that TL is insensitive to the sound-speed variations during the experiment. Using the normal-mode propagation code, one finds that the receiver to be in the "shadow zone" when the source-receiver range is approximately 3 to 5.5 km; in this range, the received level will be sensitive to (variations in) the sound speed-profile. Using the PE model, the shadow zone structure changes somewhat. Otherwise, there is an overall agreement in the TL prediction of the two models. (The specific details of TL will usually differ between the PE and normal mode calculations). We note that the model results are to be used only for the assumed acoustic environments. There are differences in the model predictions, such as the presence or absence of the shadow zones, which are not very well understood. Thus

experimental checking of the model predictions becomes important. We note that these (full field) models have been numerically bench marked (compared with each other) and extensively tested with data at low frequencies. Similar effort is lacking at mid/high frequencies. LWAD will provide excellent data for model comparisons and for evaluating the TL prediction capability of Navy systems, if the relevant issues are carefully examined.

5. ACKNOWLEDGMENT

This work is supported by the Office of Naval Research under the Littoral Warfare Advanced Development program.

6. REFERENCES

1. J. Levinson et al. "An efficient and robust method for underwater acoustic normal-mode computation," J. Acoust. Soc. Am. 97, 1576-1585 (1995).
2. J. Bucca and J. K. Fulford, "Environmental Variability During the Littoral Warfare Advanced Development Sponsored Focused Technology Experiment (FTE 96-1) Exercise, NRL Memorandum Report 7182-96-8014, 1996.
3. Smith, "UMPE: The University of Miami Parabolic Equation Model," MPL Report 432, Scrips Institute of Oceanography, Univ. of San Diego, 1993.
4. Athanasios Papoulis, "Probability, Random Variables, and Stochastic Processes", second edition, McGraw-Hill, 1984.

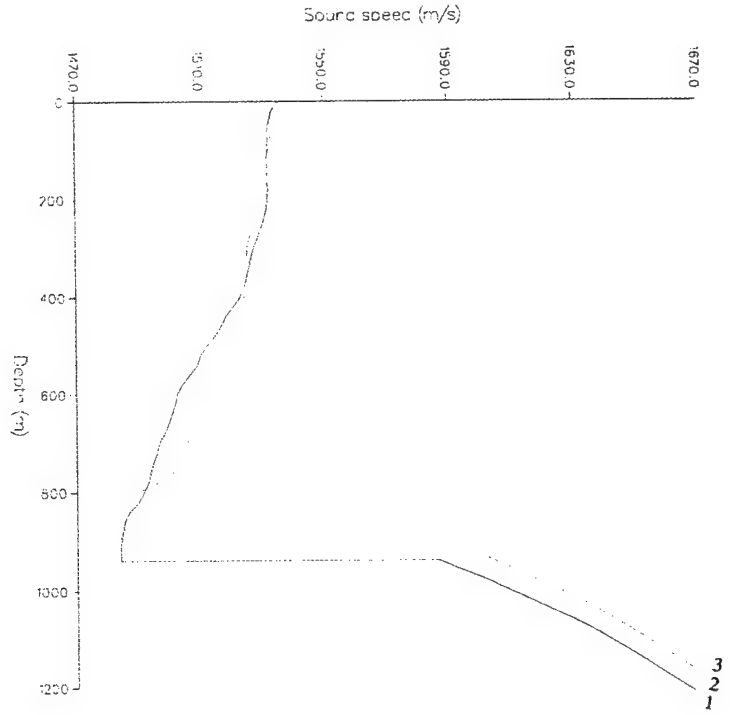

Fig. 1 — Three sound speed profiles measured during the FTE 96-1 experiment.

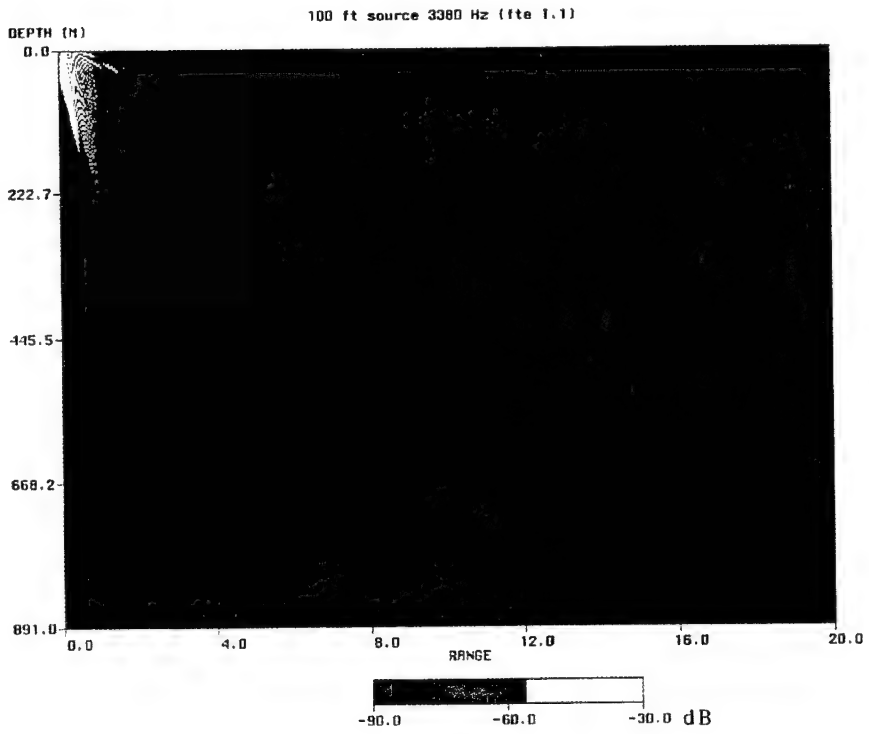

Fig. 2 — The acoustic field for a source at a depth of 30.5 m (100 ft), with 0 dB source level as a function of receiver depth and range using the first sound speed profile of Fig. 1.

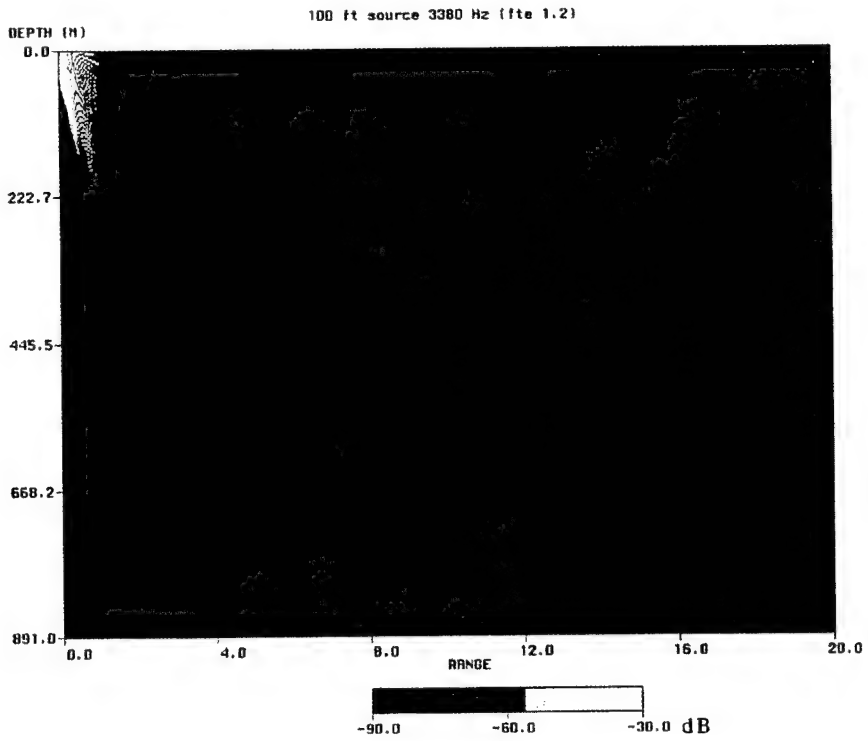

Fig. 3 — The acoustic field for a source at a depth of 30.5 m (100 ft), with 0 dB source level as a function of receiver depth and range using the second sound speed profile of Fig. 1.

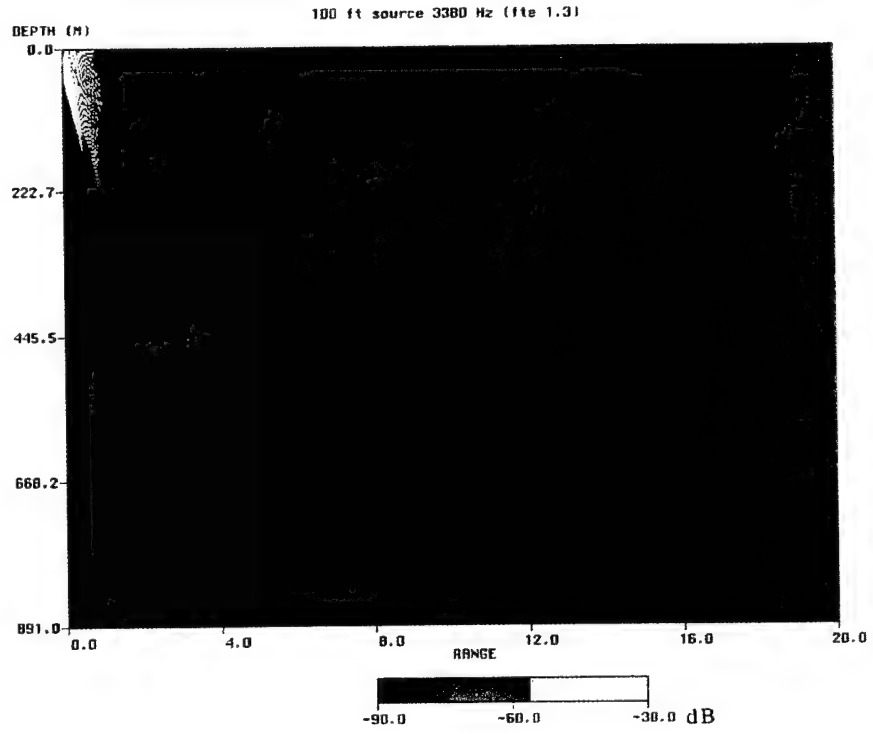

Fig. 4 — The acoustic field for a source at a depth of 30.5 m (100 ft), with 0 dB source level as a function of receiver depth and range using the third sound speed profile of Fig. 1.

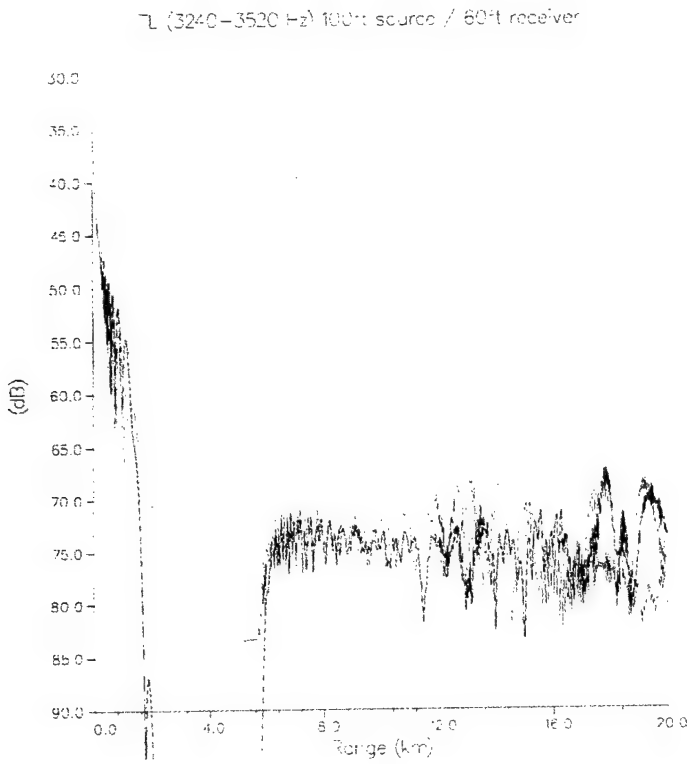

a

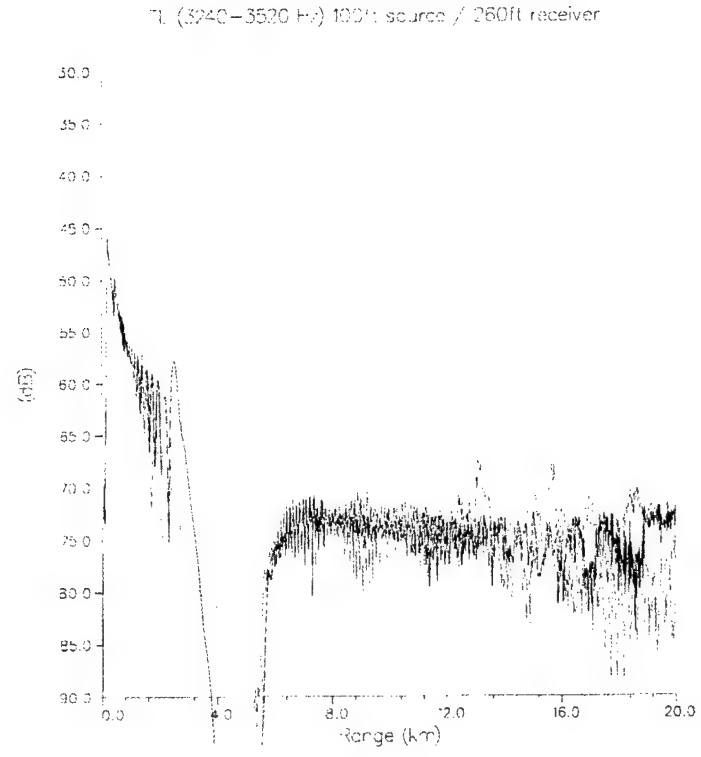

b

Fig. 5 — The modeled TL as a function of range for a source at a depth of 30.5 m (100 ft). The receiver is at a depth of 18.3 m (60 ft), (a) and 79.3 m (260 ft), (b).

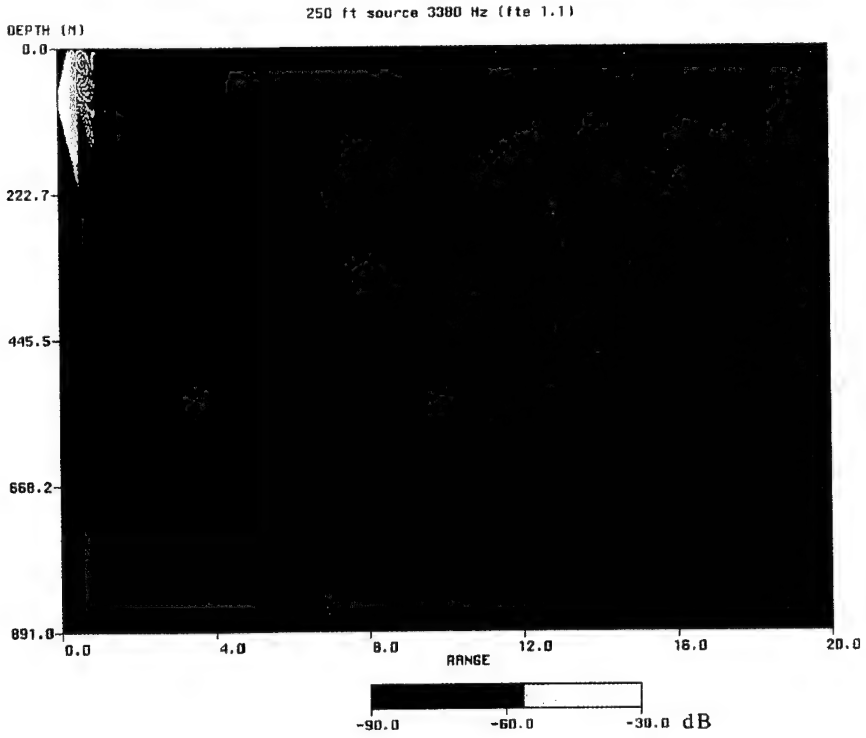

Fig. 6 — The acoustic field for a source at a depth of 76.2 m (250 ft), with 0 dB source level as a function of receiver depth and range using the first sound speed profile of Fig. 1.

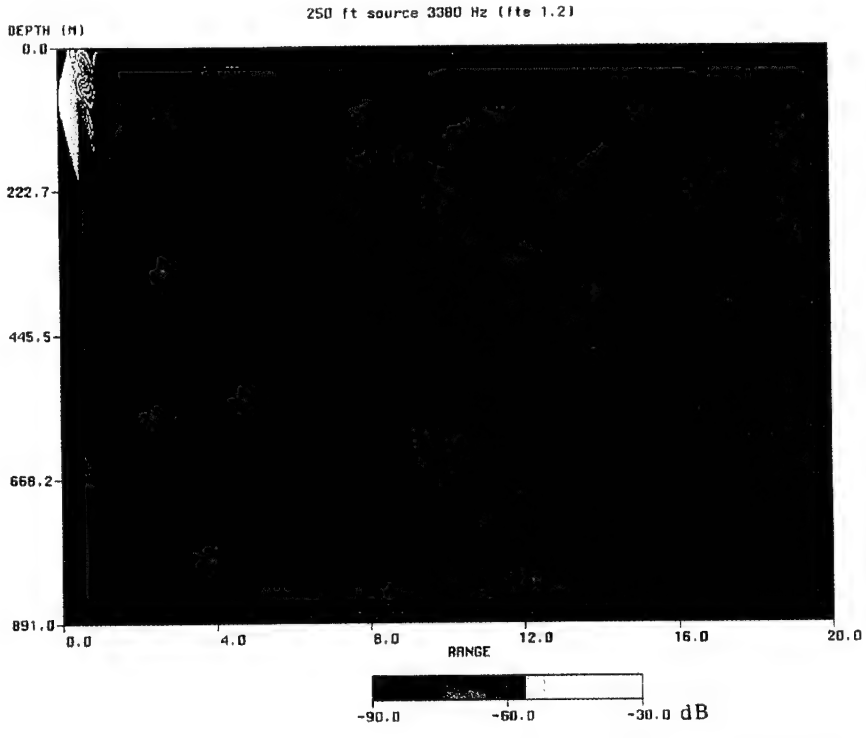

Fig. 7 — The acoustic field for a source at a depth of 76.2 m (250 ft), with 0 dB source level as a function of receiver depth and range using the second sound speed profile of Fig. 1.

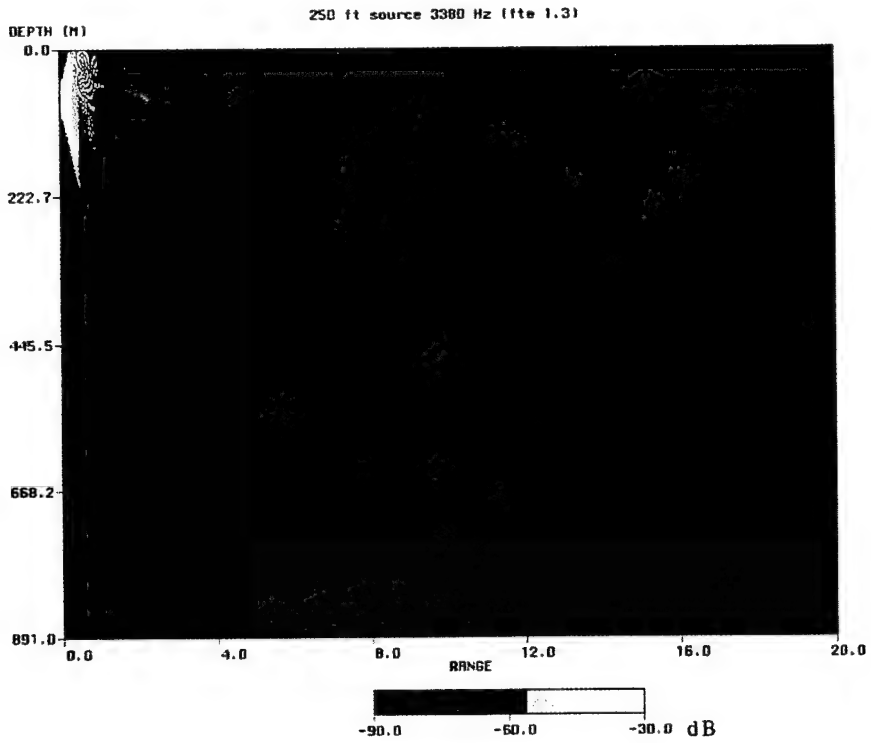

Fig. 8 — The acoustic field for a source at a depth of 76.2 m (250 ft), with 0 dB source level as a function of receiver depth and range using the third sound speed profile of Fig. 1.

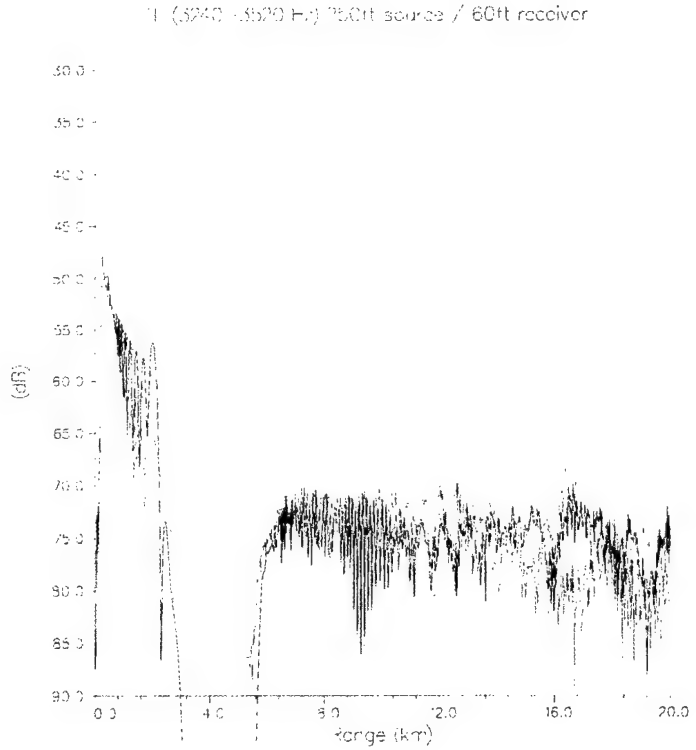

Fig. 9(a) — The modeled TL as a function of range for a source at a depth of 76.2 m (250 ft). The receiver is at a depth of 18.3 m (60 ft).

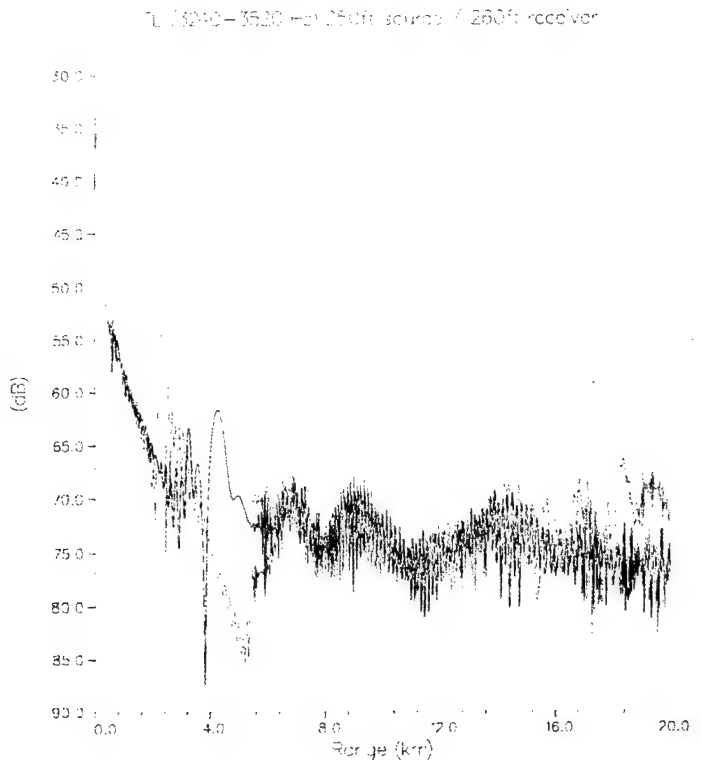

Fig. 9(b) — Same as Fig. 9(a) with the receiver at a depth of 79.3 m (260 ft).

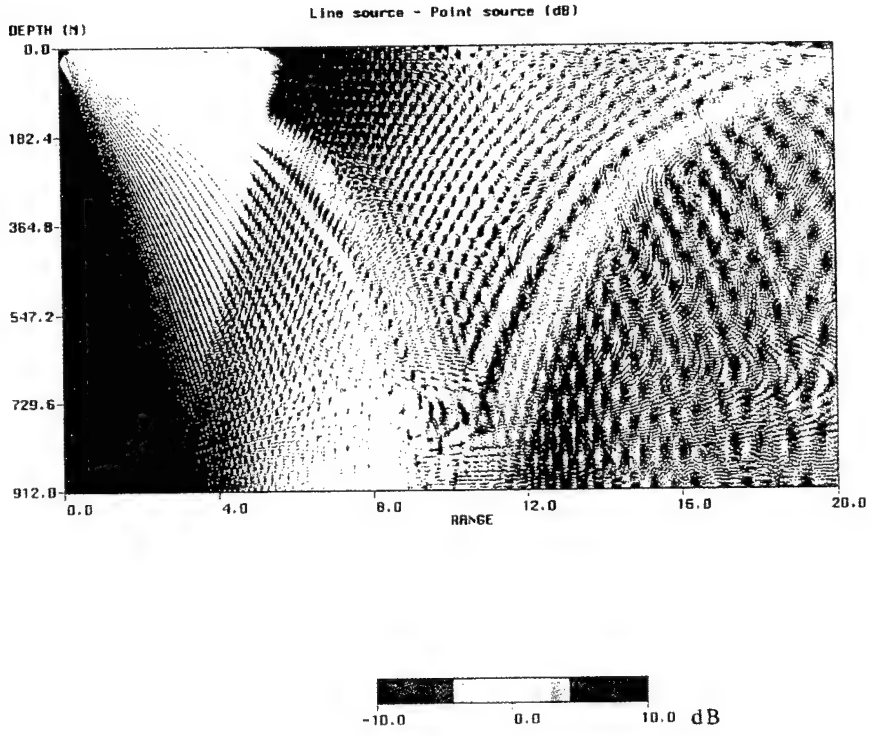

Fig. 10 — The dB difference of the normalized intensity of the line source and a point source.

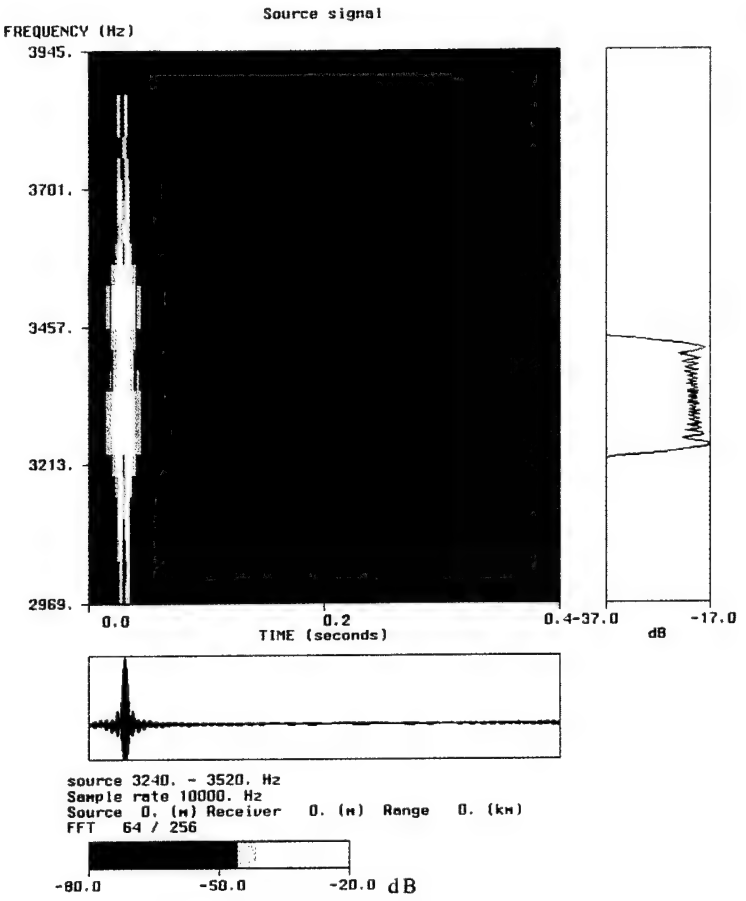

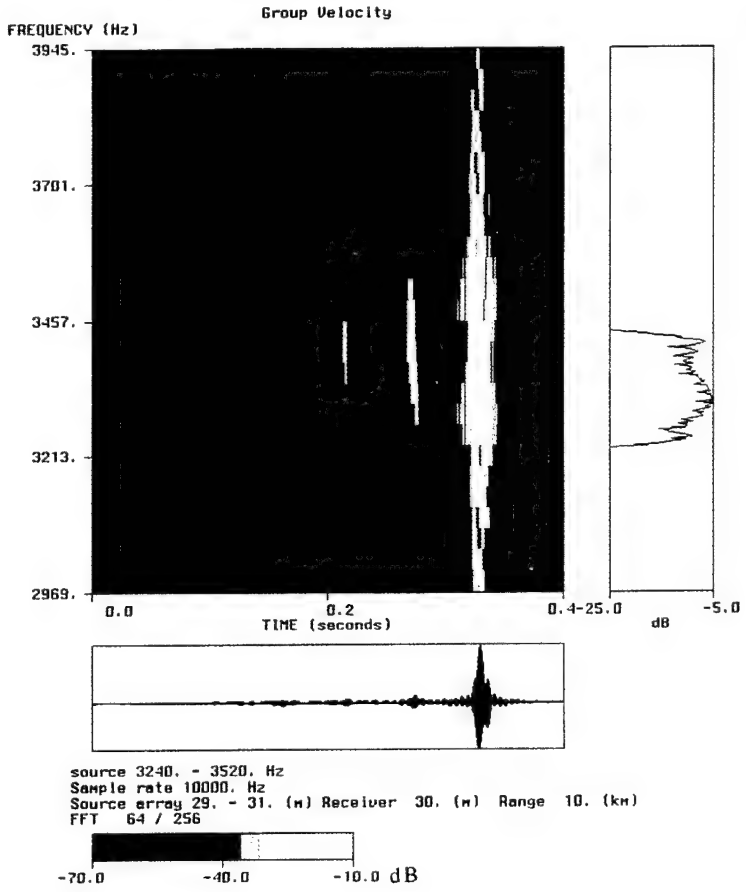

Fig. 11 — The matched filter output of an HFM signal of 512 msec duration, ~200 Hz bandwidth projected at the source (a) and received at a range of 10 km (b). The spectrum of the signal and its time-frequency dispersion are also shown at the source and receiver location. The intensities are in an arbitrary scale.

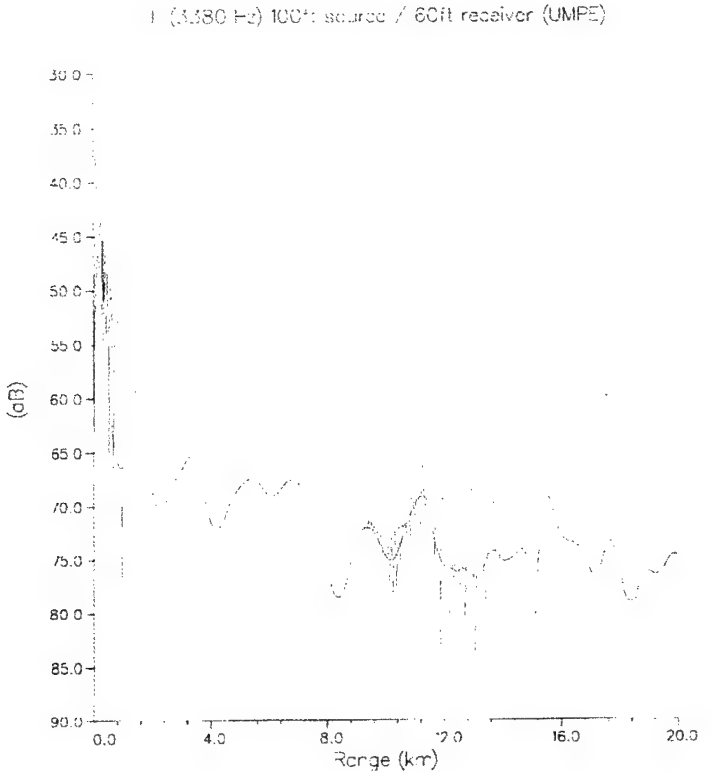

a

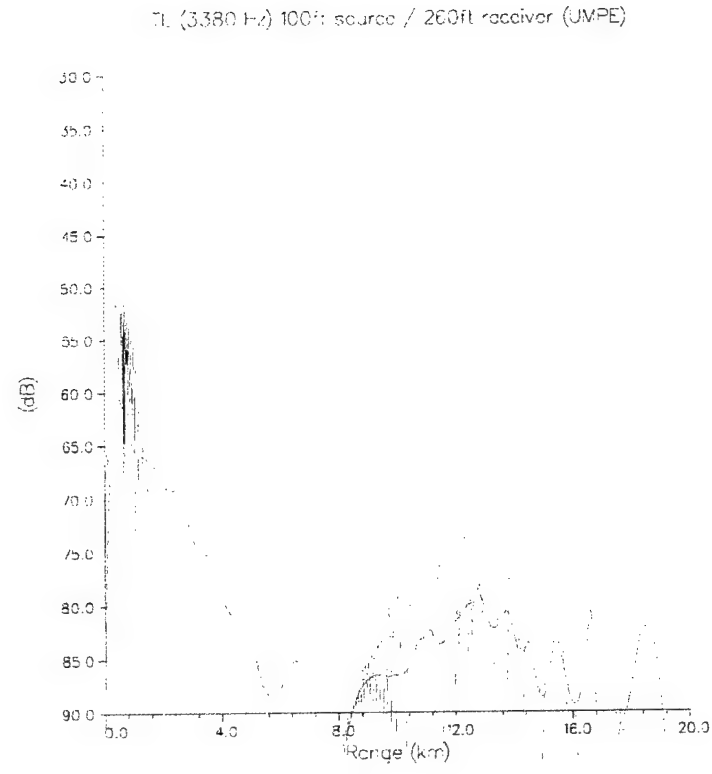

b

Fig. 12 — Transmission loss calculated using UMPE for a 30.5 m (100 ft) source and two receivers at depths of 18.3 m (60 ft) (a) and 79.26 m (260 ft) (b). The blue curve represents the range averaged (TL) values of the red curve.

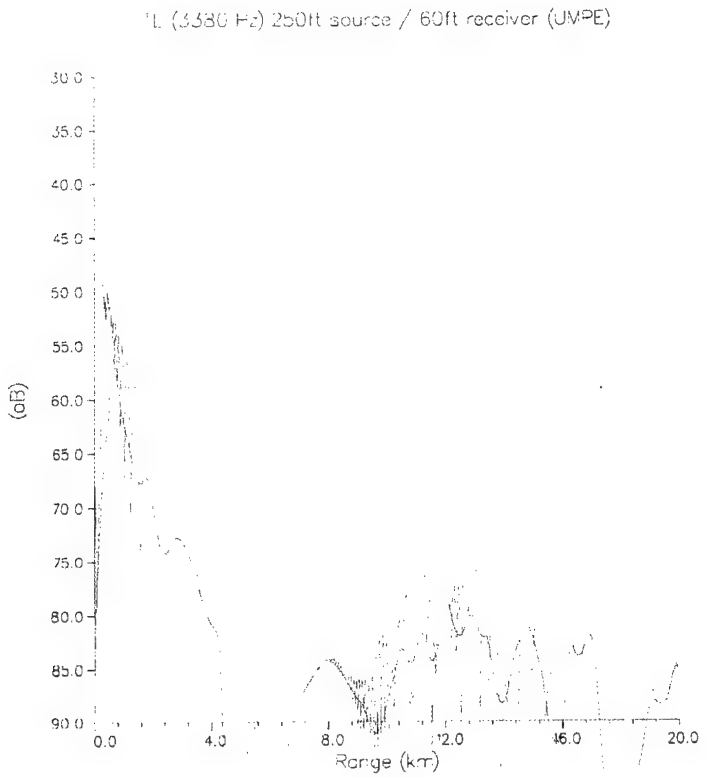

a

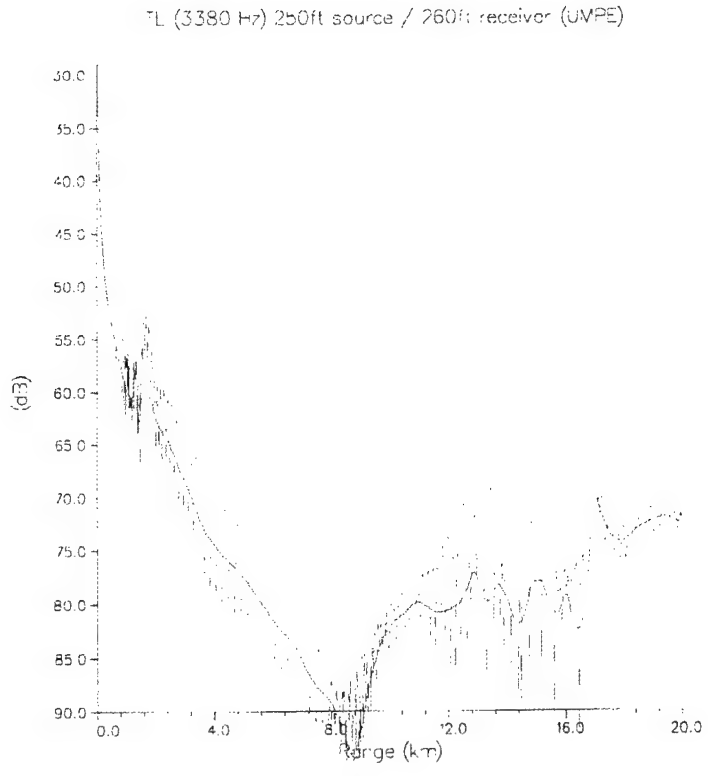

b

Fig. 13 — Transmission loss calculated using UMPE for a 76.2 m (250 ft) source and two receivers at depths of 18.3 (60 ft) (a) and 79.26 m (260 ft) (b). The blue curve represents the range averaged (TL) values of the red curve.

Appendix A

Measurement of TL and Channel Transfer Function using Coherent Broadband Waveforms

Traditionally, transmission loss (TL) at a fixed frequency has been measured using a CW source. Explosive charges have been used for wide-band TL measurements. Recently, TL measurements have been conducted using coherent wide-band waveforms. This allows the estimation of the TL and the study of multi-path propagation without the need for a high level source. The multi-path arrival structure estimation is important for identifying echoes in an active system. The ability to estimate the channel transfer function (within the signal bandwidth) using a coherent waveform is a significant advantage.

This appendix discusses briefly the advantages and disadvantages of the above methods. The primary purpose of this appendix is to illustrate the coherent wide-band waveforms that are used in the LWAD experiments, and how the broadband data will be processed to estimate the TL and channel transfer function when the received data have low signal-to-noise ratio (SNR).

A 1. Narrow-band versus Broadband Sources

A narrow-band source is commonly used for TL measurements. A narrow-band CW source is normally well calibrated. It can be towed at a depth and yields TL as a function of range. There may be practical difficulties in shallow water at tactical frequencies. In shallow water, due to the high TL at tactical frequencies, a source of high (greater than 190 dB// μPa at 1 m) level would be required. Such a source can be expensive. Also, the medium fluctuation may limit the processing gain at the receiver side. To improve the SNR of the received signal, narrow-band processing has been applied to the CW data which assumes a stable tone over the processing time window. The Doppler shift due to scattering from surface waves, currents, and unknown source motion could significantly modify the signal. Severe Doppler shift/spread would limit the maximum length of the time window and hence limit the processing gain.

Explosive charges are widely used for broadband TL measurements at low frequencies (source level decreases significantly at high frequencies. The explosive charges are normally detonated at a series of ranges to get the range dependence of the TL. The signal energy is integrated over a wide bandwidth to estimate the broadband TL. The source level of explosive charges are low at tactical frequencies and the source spectra (level) are not (exactly) repeatable primarily because of depth variations. These shortcomings of explosive sources present difficulties for TL measurement at tactical frequencies.

Coherent broadband waveforms, such as the M-sequence which is a pseudo-random broadband waveform, are used in many acoustic experiments. It is sufficient to use a relatively low level

broadband source with long signal duration (on the order of seconds). The received signal is passed through a matched filter to enhance the SNR. Other coherent broadband waveforms, such as the LFM signals, are used by active systems which also use matched filter processing to enhance the SNR at the receiver. Coherent broadband waveforms can be used to estimate the channel transfer function as well as the TL. Note that broadband TL is the power spectrum level of the transfer function averaged over the frequency band.

There are several issues related to using coherent broadband waveforms. The first has to do with the coherent frequency bandwidth of the signal which is not well known. One basically assumes that the coherent bandwidth supported by the channel is larger than the bandwidth of the actual signal used. The second has to do with effectiveness of the matched filter when there is frequency dispersion and signal distortion due to multi-path structure and random fluctuations in the ocean. The effect of the multi-paths and frequency dispersion can be studied using simulations as illustrated below. The effect of the random fluctuations can be studied by comparing the data with the (deterministic) simulation results. The latter is an interesting topic in its own right.

A 2. Coherent Broadband Waveforms

The broadband waveform is constructed as a succession of segments, see Fig. A-1. A segment can be made, for example, of 4 seconds signal and 2 seconds of silence, as shown in Fig. A-2.

FIGURE A-1. The succession of segments that comprise the broadband signal.

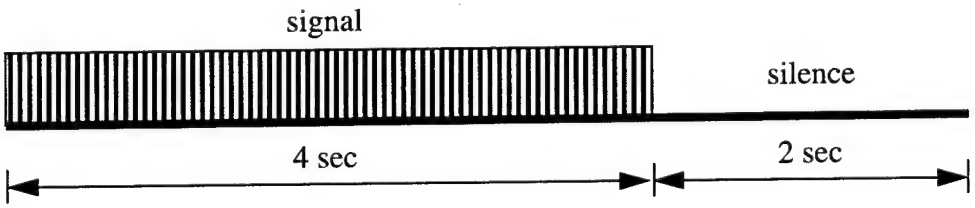

FIGURE A-2. A segment of the broadband signal.

The LFM signal is generated according to the formula,

$$S(t) = A\exp\left[j2\pi\left(f_1 t + \left((f_2 - f_1)\,t^2\right)/T\right)\right] \qquad \text{(EQ A-1)}$$

where, $f_1 = F_c - F_{sw}/2$, $f_2 = F_c$, T is the pulse period, F_c is the carrier frequency, F_{sw} is the width of the frequency sweep. In this study, the frequency sweep is 1 k Hz centered at 3.5 kHz.

A pseudorandom number generator is used to create a PRN signal with 500 Hz bandwidth centered at 3.5 kHz carrier frequency.

A 3. Processing of Broadband Waveforms

A coherent broad-band waveform can yield a larger processing gain than that of a CW signal of the same duration. As is well known, a CW signal is enhanced (over white noise) in the frequency domain by a processing gain of 10logT, where T is the signal duration in seconds. A coherent broad-band waveform of bandwidth W and duration T can be enhanced by a matched filter by as much as 10logWT. A coherent broad-band waveform will be processed using the matched filter as depicted in Fig. A-3. The matched filter in this case is the time reversed original transmitted signal. The matched filter serves two purposes. It functions as a bandpass filter which eliminates the noise outside the signal band. Also, it compresses the signal in a time window T to a sharp impulse. The time compression allows a low level source to be used for TL measurements. The processing gain is illustrated here and the estimation of TL using a broadband waveform is illustrated in the next section.

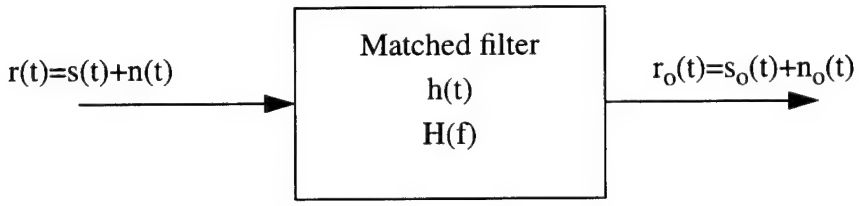

FIGURE A-3. Matched filter block diagram

As addressed in various textbooks[4], the matched filter yields the following output SNR,

$$\left(\frac{S}{N}\right)_{out} = \frac{s_o^{\,2}(t_o)}{\langle n_o^{\,2}(t)\rangle}, \qquad \text{(EQ A-2)}$$

The matched filter is represented in the frequency domain by

$$H(f) = K\frac{S^*(f)}{P_n(f)}e^{-j2\pi f t_o}, \qquad \text{(EQ A-3)}$$

where $S(f) = F[s(t)]$ is the Fourier transform of the known input signal $s(t)$ of duration T sec. $P_n(f)$ is the PSD of the input noise n(t), t_o is the sampling time when $(S/N)_{out}$ is evaluated, and K is an arbitrary real nonzero constant.

For the case of white noise, the description of the matched filter is simplified as follows. Assuming that $P_n(f) = \frac{N_o}{2}$, then

$$H(f) = 2K\frac{S^*(f)}{N_o}e^{-j2\pi f t_o}. \quad \text{(EQ A-4)}$$

Therefore, when the input noise is white, the time domain representation of the matched filter becomes

$$h(t) = Cs(t_o - t) \quad \text{(EQ A-5)}$$

where $C = 2K/N_o$.

Notice that

$$s_o(t_o) = \int_{-\infty}^{\infty} H(f)\,S(f)\,e^{-j2\pi f t_o}df. \quad \text{(EQ A-6)}$$

Using Parseval's theorem we get

$$\left(\frac{S}{N}\right)_{out} = \int_{-\infty}^{\infty}\frac{|S(f)|^2}{N_o/2}df = \frac{2}{N_o}\int_{-\infty}^{\infty}s^2(t)\,dt, \quad \text{(EQ A-7)}$$

but $\int_{-\infty}^{\infty}s^2(t)\,dt = E_s$ is the energy in the finite-duration input signal. Thus

$$\left(\frac{S}{N}\right)_{out} = \frac{2E_s}{N_o} \quad \text{(EQ A-8)}$$

This is a very interesting result. it states that the $(S/N)_{out}$ depends on the signal energy and PSD level of the noise and not on the particular signal waveform used.

Equation A-8 can also be written in terms of a time-bandwidth product and the ratio of the input average signal power (over T sec) to average noise power. Assume that the input noise power is measured in a band that is W hertz wide. Also, the known signal has a duration of T seconds. Then

$$\left(\frac{S}{N}\right)_{out} = 2TW\frac{(E_s/T)}{N_o W} = TW\left(\frac{S}{N}\right)_{in} \quad \text{(EQ A-9)}$$

where $\left(\frac{S}{N}\right)_{in} = \frac{(E_s/T)}{WN_o/2}$. This result shows that it is desirable to have an input signal and noise with large time-bandwidth product. For the numerical example, we use a 4 seconds LFM signal with bandwidth of 1 kHz, and centered at 3.5 kHz. The time series of this LFM waveform is shown in Fig. A-4, and its spectrum is shown in Fig. A-5. We add to this signal a Gaussian white noise of RMS intensity equals that of the signal. The noise time series is shown in Fig. A-6. The signal-to-noise ratio is 0 dB.

Figure A-7 shows the output signal plus noise after the matched filter. This signal is now seen as an impulse with high SNR. Fig. A-7 shows the signal and noise intensity in dB in order to illustrate the processing gain. We find that the output SNR is about 36 dB which is what expected from Eq. A-9. The noise RMS level is estimated using noise outside the signal band.

A 4. Estimation of the Channel Transfer Function and TL

In this section, we illustrate how the channel impulse response and TL can be estimated from the received data of a broadband waveform. The same LFM waveform as described above is transmitted. The received waveform is simulated by convolving the channel "impulse response" with the transmitted signal. The received waveform, generally, will have low (or negative) SNR. The channel transfer function and TL are deduced from the received data.

The oceanic channel impulse response is generated using a modified version of the University of Miami broadband PE (UMPE) model. The channel impulse response is plotted in Fig. A-8. For this example, a sound-speed profile similar to FTE 96-1 environment is used. The source-receiver separation is 5 km and both are at a depth of 10 m.

Figure A-9 shows the estimated channel impulse response. We find that the estimated channel impulse response is very similar to the original channel impulse response within a scaling factor.

Fig. A-10 shows the received (raw) data, where white Gaussian noise is added to it. The raw data have a SNR of approximately 10 dB. We use small positive SNR in order to show the signal. Figure A-11 shows the received signal at the output of the matched filter. Note that Fig. A-11 contains the channel impulse response which is shown in Fig. A-9 with an expanded time scale.

Figures A-12(a) and 12(b) show the PSD of the transmitted signal, Fig. A-5, and the received matched filtered signal, Fig. A-11. The average TL in the signal band is about 55 dB.

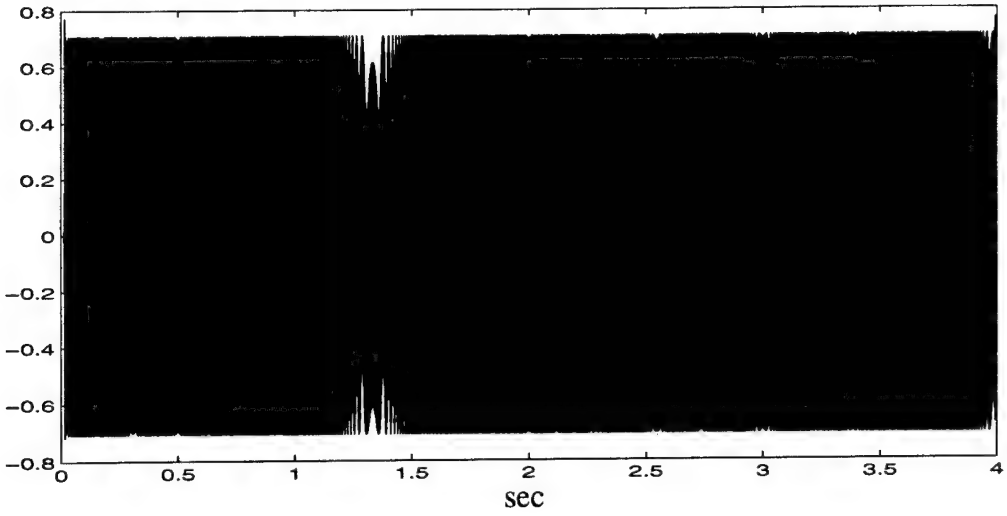

FIGURE A-4. Time series of the LFM signal with sweep of 1 kHz centered around 3.5 kHz.

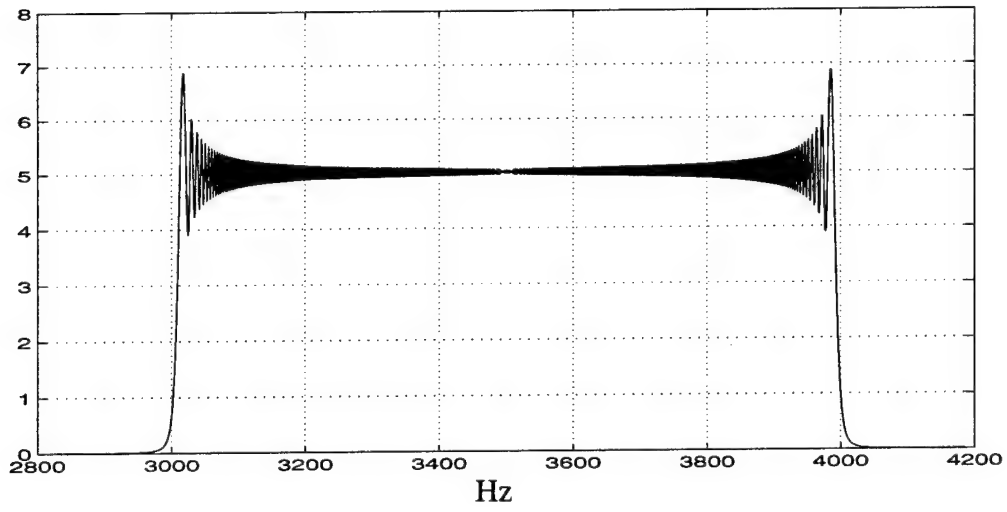

FIGURE A-5. The spectra of the LFM signal.

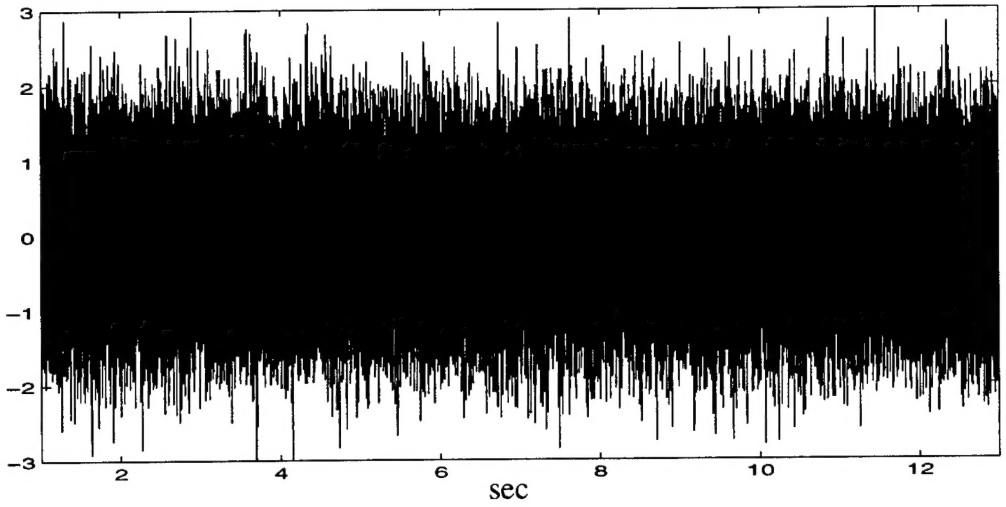

FIGURE A-6. Time series of the white Gaussian noise.

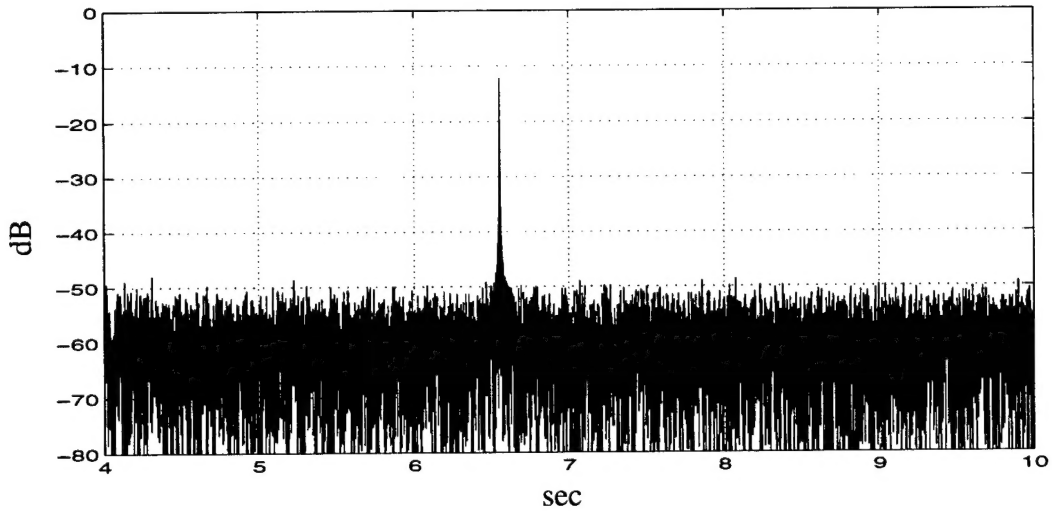

FIGURE A-7. The LFM signal plus noise at the output of the matched filter,

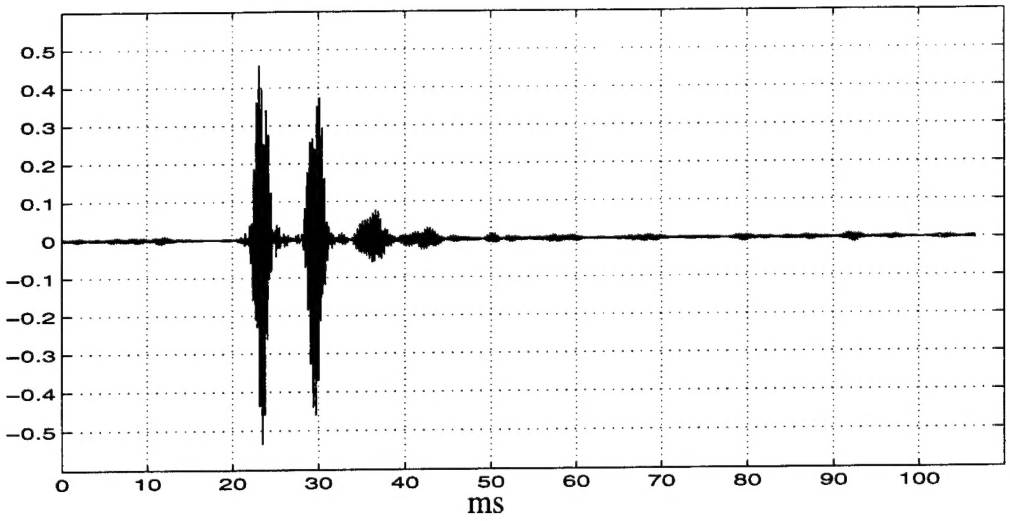

FIGURE A-8. The impulse response of the oceanic channel generated by a broadband PE code.

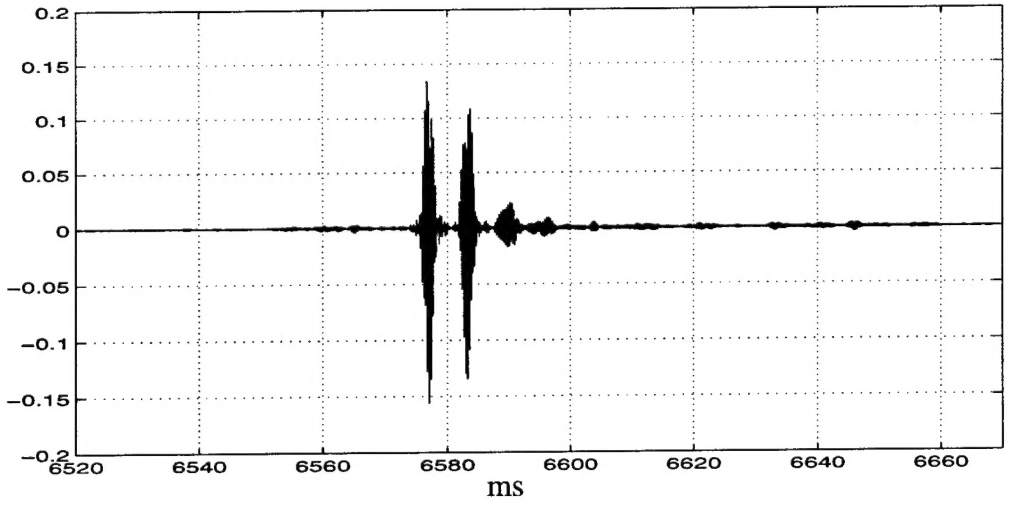

FIGURE A-9. The estimated channel impulse response.

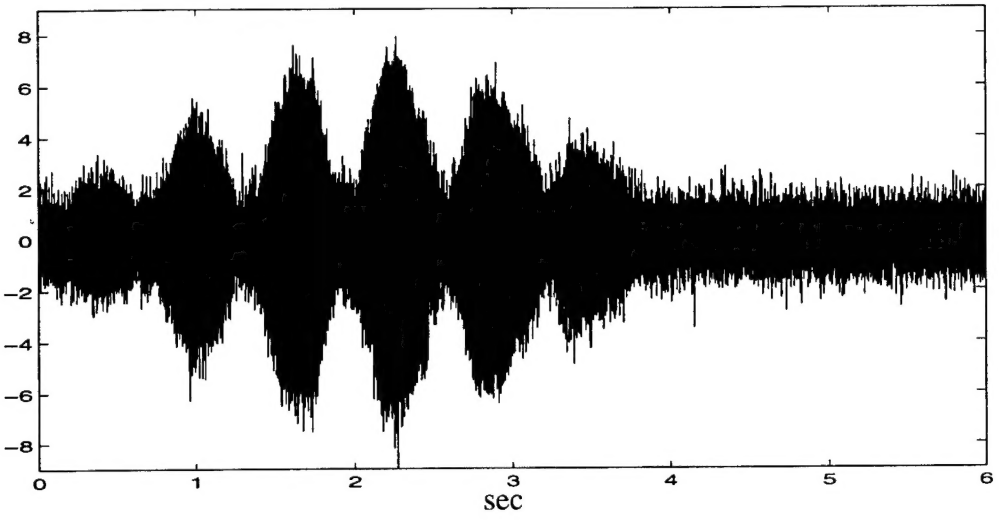

FIGURE A-10. The received signal plus the additive noise.

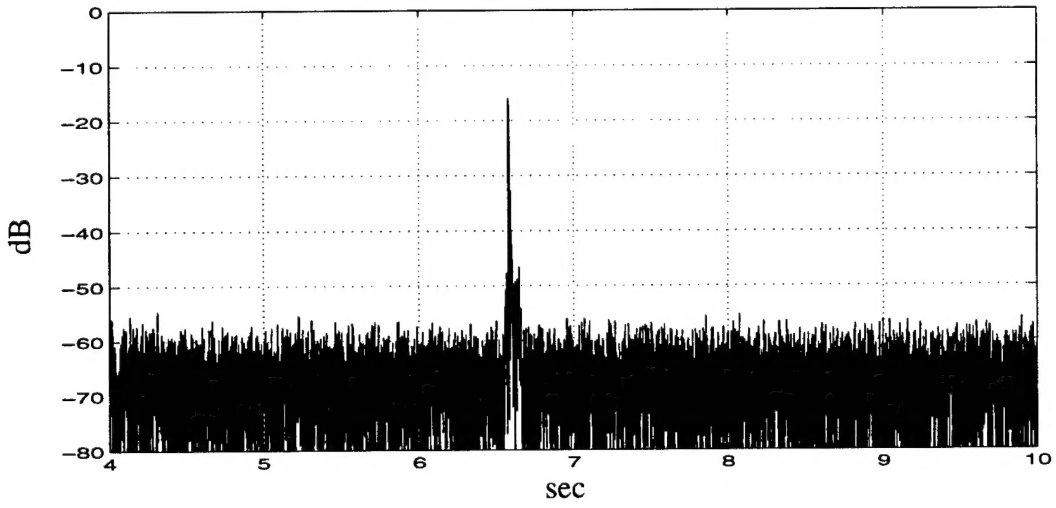

FIGURE A-11. The received and matched filtered signal.

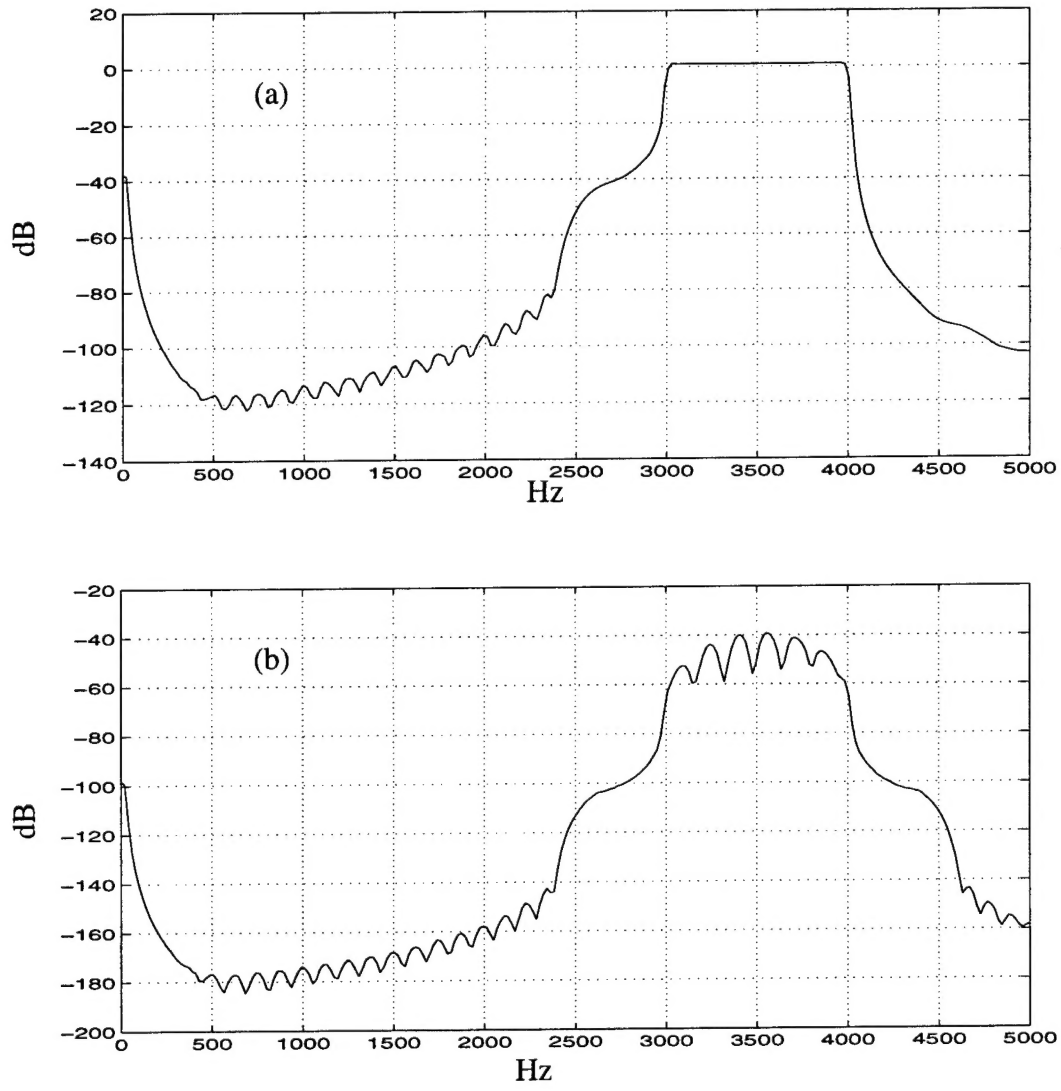

FIGURE A-12. PSD of the LFM (transmitted) signal (a), and the received signal at the output of the matched filter (b).